Published for SISSA by Springer

Received: *January 1, 2022*
Revised: *April 23, 2022*
Accepted: *May 10, 2022*
Published: *June 13, 2022*

Damping signatures at JUNO, a medium-baseline reactor neutrino oscillation experiment

The JUNO collaboration

E-mail: Juno_pub_comm@juno.ihep.ac.cn

Abstract: We study damping signatures at the Jiangmen Underground Neutrino Observatory (JUNO), a medium-baseline reactor neutrino oscillation experiment. These damping signatures are motivated by various new physics models, including quantum decoherence, ν_3 decay, neutrino absorption, and wave packet decoherence. The phenomenological effects of these models can be characterized by exponential damping factors at the probability level. We assess how well JUNO can constrain these damping parameters and how to disentangle these different damping signatures at JUNO. Compared to current experimental limits, JUNO can significantly improve the limits on τ_3/m_3 in the ν_3 decay model, the width of the neutrino wave packet σ_x, and the intrinsic relative dispersion of neutrino momentum $\sigma_{\rm rel}$.

Keywords: Neutrino Detectors and Telescopes (experiments)

ArXiv ePrint: 2112.14450

https://doi.org/10.1007/JHEP06(2022)062

Contents

1 Introduction

Neutrino oscillation was first proposed by Bruno Pontecovero in 1957 [1] and was invoked for the solution of atmospheric neutrino anomaly and solar neutrino puzzle. It was experimentally confirmed by the Super-Kamioka Neutrino Detection Experiment (Super-K, SK) [2] in 1998 and the Sudbury Neutrino Observatory (SNO) [3] in 2002; for further details see ref. [4]. Most neutrino oscillation experiments can be well explained in the Standard Model (SM) with three massive neutrinos. In the standard three-flavor neutrino oscillation framework, the three known neutrino flavor eigenstates (ν_e, ν_μ, and ν_τ) can be written as quantum superpositions of three mass eigenstates (ν_1, ν_2, and ν_3), and the neutrino oscillation probabilities are expressed in terms of six oscillation parameters: three mixing angles (θ_{12}, θ_{13}, and θ_{23}), two mass-squared differences (Δm^2_{21} and Δm^2_{31}), and one Dirac CP phase ($\delta_{\rm CP}$). The Majorana CP phases play no role in neutrino oscillations if neutrinos are Majorana particles. Among these six observable oscillation parameters, Δm^2_{21}, $|\Delta m^2_{31}|$, θ_{12}, and θ_{13} have been well determined to the few-percent level. However, the neutrino mass ordering (whether Δm^2_{31} is positive or negative), the octant of θ_{23} (whether θ_{23} is larger or smaller than 45°) and the Dirac CP phase are still open questions. At present, the normal mass ordering (NMO) and the second octant of θ_{23} are both favored by less than 3σ confidence level (CL) [4–6], and $\delta_{\rm CP}$ is in the range of [-3.41, -0.03] for the NMO and [-2.54, -0.32] for the inverted mass ordering (IMO) at the 3σ CL [7], respectively. The main physics goals of next-generation neutrino oscillation experiments, such as the

Deep Underground Neutrino Experiment (DUNE) [8, 9], Hyper-Kamiokande [10] and the Jiangmen Underground Neutrino Observatory (JUNO) [11, 12], are to determine the mass ordering with a $3-5\sigma$ CL and to observe CP violation with a 3σ CL for $\sim 75\%$ of $\delta_{\rm CP}$ values, etc. To reach these goals, the ability to achieve high-precision measurement of the oscillation spectrum is required for these experiments. In the meantime, these high-precision experiments will also reach sufficient sensitivity to probe new physics beyond the standard three-neutrino paradigm.

The presence of new physics in the neutrino sector would yield corrections to the standard three-flavor neutrino oscillation probabilities, thus leading to modifications to the spectrum measured in high-precision neutrino oscillation experiments. Among various possible new physics scenarios, a number of them lead to exponential damping in the neutrino oscillation probabilities [13, 14], which could yield a different number of neutrinos observed than expected [14–19] or a shift in the best fit values for neutrino oscillation parameters [13–17, 20–25]. These damping signatures can be treated as secondary effects relative to the standard three-neutrino oscillations in the neutrino flavor transitions. In this work, we present a systematic study of the possible damping effects at the JUNO detector. JUNO is a medium-baseline reactor neutrino experiment with a 20kton liquid scintillator (LS) detector located in a laboratory at 700m underground in Jiangmen, China. The main physics goals of JUNO are to determine the mass ordering and perform high-precision measurements of the neutrino oscillation parameters $\sin^2\theta_{12}$, Δm^2_{21} and $|\Delta m^2_{ee}|$ [11, 12]. Also, JUNO is expected to be sensitive to the tiny damping signatures due to its effective energy resolution of 3% at 1 MeV and the capability of measuring multiple oscillation cycles [25].

This paper is organized as follows. In section 2, we discuss the damping signatures arising from different new physics models. In section 3, we discuss the damping signatures at medium-baseline reactor neutrino experiments. In section 4, we describe the statistical analysis method for JUNO used in this work. In section 5, we present the results of constraining and disentangling damping signatures at JUNO. We conclude in section 6.

2 Damping signatures from new physics models

Damping signatures can be induced by a class of new physics models. Here, we focus on the exponential damping framework [13, 14], i.e., they can be written in the form of multiplying each term of the neutrino oscillation probabilities with exponential factors, which can arise from an approximation of the first- or second-order perturbations to the standard neutrino oscillation probabilities from new physics scenarios [25–27]. In this framework, the general expression for the probability of ν_a oscillating into ν_b in vacuum is given by

$$P(\nu_a \to \nu_b) = \sum_{\rm i,j=1}^{3} U_{a\rm j} U^*_{b\rm j} U^*_{a\rm i} U_{b\rm i} \exp\left(-\mathbf{i}\frac{\Delta m^2_{\rm ij} L}{2E}\right) D_{\rm ij}(\alpha_{\rm ij}), \tag{2.1}$$

where U is the Pontecorvo-Maki-Nakagawa-Sakata (PMNS) mixing matrix [3, 4], $\Delta m^2_{\rm ij} = m^2_{\rm i} - m^2_{\rm j}$, with $m_{\rm i}$ being the eigenstate mass of $\nu_{\rm i}$; L is the baseline length, E is the neutrino energy; $D_{\rm ij}$ is an exponential damping factor and the specific form can be found in table 1,

Type	Damping effect	Reference	Damping factor $D_{\rm ij}$	Units of α
(1)	QD I	[20, 23, 28–33]	$\exp(-\alpha L/E^2)$	$\text{MeV}^2\cdot\text{m}^{-1}$
(2)	QD II	[20, 23, 28–40]	$\exp(-\alpha L)$	m^{-1}
(3)	QD III	[13, 20, 23, 28–33, 35–39]	$\exp(-\alpha LE^2)$	$\text{MeV}^{-2}\cdot\text{m}^{-1}$
(4)	Absorption	[13, 20, 23, 28–32, 40]	$\exp(-\alpha LE)$	$\text{MeV}^{-1}\cdot\text{m}^{-1}$
(5)	ν_3 decay	[15–17, 19, 41–43]	$\left\{\exp\left(-\alpha\frac{L}{E}\right),\ \exp\left(-\alpha\frac{L}{2E}\right)\right\}$	$\text{MeV}\cdot\text{m}^{-1}$
(6)	WPD I	[13, 23, 24, 44–49]	$\exp\left(-\alpha\frac{(\Delta m^2_{\rm ij})^2L^2}{E^4}\right)$	MeV^2
(7)	WPD II	[13, 25, 37, 50]	$\exp\left(-\alpha\frac{(\Delta m^2_{\rm ij})^2L^2}{E^2}\right)$	dimensionless
(8)	WPD III	[21, 22, 25, 51, 52]	$\exp(-R-\mathbf{i}X)$	dimensionless

Table 1. List of new physics models with different exponential damping factors. The definitions of the parameters in the type (8) model are given in eq. (2.2).

and the $\alpha_{\rm ij}$ are damping coefficients. Hereinafter, except for the ν_3 decay case, we assume universal couplings, i.e., $\alpha_{\rm ij}\equiv\alpha$, to describe the magnitudes of different damping effects.

The damping signatures from various new physics models are summarized in table 1. These models include quantum decoherence (QD), neutrino absorption, ν_3 decay, and wave packet decoherence (WPD). The new physics models of types (1) – (5) in table 1 are expressed as power-law dependencies of the exponential form, i.e., $\exp(-\alpha LE^n)$ with $n=0$, ±1, and ±2 [20, 23, 28–33, 35, 37, 39, 40]. Specifically, the type (1) model ($n=-2$) is demonstrated in ref. [20] that it has the same functional form as the effects induced by stochastic density fluctuations. Thus, it is used to probe QD effects that might be induced by matter density fluctuations. The corresponding constraints of this model can be interpreted as limits on possible matter density fluctuations in the Sun [20]. The most significant feature of the type (2) model ($n=0$) is independent of neutrino energy. Many researchers have focused on this model since it is the simplest case of QD effects that might be induced by quantum gravity [20, 23, 28–40]. The type (3) model ($n=2$) is used to probe QD effects that might be induced by the space-time “foam” configurations of quantum gravity or D-brane of the form $\alpha\propto E^2/M_{\rm Planck}$ [20, 35, 53, 54], where $M_{\rm Planck}$ is the Planck mass scale. The type (4) model ($n=1$), which is called neutrino absorption in ref. [13], is used to describe the absorption effect when neutrinos propagate through matter. In this type of model, $\alpha\equiv\rho\sigma(E_0)/E_0$, where ρ is the matter density and $\sigma(E_0)$ is the effective cross section for neutrinos with an energy of E_0. Currently, neither atmospheric, solar neutrino oscillation experiments nor the long-baseline reactor neutrino experiment Kamioka Liquid Scintillator Anti-Neutrino Detector (KamLAND) shows evidence in favor of the new physics effects described by the previous four models ($n=0$, 1 and ±2) [20, 35], which also indicates that their damping parameter α can be strongly constrained. Furthermore, there are no significant changes in the best-fit neutrino oscillation parameters in these new physics scenarios [30, 31, 33, 40]. The fact that neutrinos are massive implies they could decay. The $n=-1$ case was used in refs. [13, 16, 18, 38, 55–62] to describe invisible neutrino decay scenarios, which lead to the violation of three-flavor neutrino unitarity. However, ref. [18] has shown that astrophysical neutrinos are potentially the most powerful source for constraining the decay parameters of ν_1 and ν_2, which could lead to the lower bounds on $\tau/m \sim 10^{-4}$ (10^6) s/eV from the solar (supernova) neutrinos. Nevertheless, the constraints on ν_3 decay is much weaker than those on ν_1 and ν_2 from the current data [16, 18, 19]. Here, in the type (5) model, we only consider the ν_3 decay scenario [15–17, 19, 41–43]. The oscillation probability of $P(\bar{\nu}_e \to \bar{\nu}_e)$ comprises two exponential forms derived from the case of $n = -1$, with α being the neutrino eigenstate mass divided by the corresponding lifetime, i.e., $\alpha \equiv m_3/\tau_3$.

Although the plane-wave approximation theory successfully interprets a wide range of neutrino experiments, it is not self-consistent and leads to many paradoxes [46, 51, 52, 63]. Therefore, the models of types (6) – (8) are proposed to form a consistent description of neutrino oscillations, which use the wave packet treatment of neutrino oscillation instead of the plane wave approximation for neutrino propagation [21, 22, 25, 46, 51, 52]. However, this description also induce some WPD effects, which have not been found in current experimental data [22, 24, 49]. Furthermore, the WPD effects and ν_3 decay can shift the best-fit neutrino oscillation parameters if these effects are strong enough [13, 16, 17, 22, 24, 49]. Specifically, the type (6) model is used to describe the decoherence effect caused by wave packet separation [13, 23, 24, 44–49]. This effect is related to the characteristics of the neutrino source and detector. In the type (6) model, $\alpha \equiv 1/(4\sqrt{2}\sigma_x)^2$, where σ_x is the spatial width of the neutrino wave packet. The type (7) model is used in ref. [50] to show that in the two-neutrino oscillation case, a Gaussian-averaged neutrino oscillation model with $\exp[-2\sigma^2(\Delta m^2)^2]$ and a neutrino decoherence model with $\exp(-d^2 L)$ are equivalent if $d = \frac{\sqrt{2}\Delta m^2}{\sqrt{L}}\sigma$ is fulfilled, where σ is the standard deviation of L/E and d is the decoherence parameter. The model with $\exp[-2\sigma^2(\Delta m^2)^2]$ is obtained by Gaussian average over the L/E dependence for the oscillation probability under the plane-wave approximation due to uncertainties in the energy and oscillation length [37, 50]. Since under the condition of $(2\sigma^2 E^4/L^2) = 1/(4\sqrt{2}\sigma_x)^2$, the type (6) and type (7) models are equivalent, we refer to the type (7) model as WPD II.

The type (8) model systematically studies the quantum decoherence effects caused by wave packet separation, dispersion and delocalization. We rewrite the unified decoherence effect in exponential form to discuss its impact on the neutrino oscillation probability. This exponential damping factor is given by [21, 22, 25, 51, 52]

$$\begin{aligned}\exp(-R-\mathbf{i}X) &= \exp\left\{-\left[\frac{1}{4}\ln(1+y_{\rm ij}^2)+\lambda_{\rm ij}+\eta_{\rm ij}\right]-\mathbf{i}\left[\frac{1}{2}\tan^{-1}(y_{\rm ij})-\lambda_{\rm ij}y_{\rm ij}\right]\right\}\\ &= \left(\frac{1}{1+y_{\rm ij}^2}\right)^{\frac{1}{4}}\exp(-\lambda_{\rm ij})\exp\left(-\frac{\mathbf{i}}{2}\tan^{-1}(y_{\rm ij})\right)\exp(\mathbf{i}\lambda_{\rm ij}y_{\rm ij})\exp(-\eta_{\rm ij}),\end{aligned} \tag{2.2}$$

where $\lambda_{\rm ij} = \frac{x_{\rm ij}^2}{1+y_{\rm ij}^2}$, $x_{\rm ij} = \frac{\sqrt{2}\Delta m_{\rm ij}^2 L}{4E}\sigma_{\rm rel}$, $y_{\rm ij} = \frac{\Delta m_{\rm ij}^2 L}{E}\sigma_{\rm rel}^2$, $\eta_{\rm ij} = \frac{1}{2}\left(\frac{\Delta m_{\rm ij}^2}{4\sigma_{\rm rel}E^2}\right)^2$, and $\sigma_{\rm rel} = (2\sigma_x E)^{-1}$. In this model, we define $\alpha \equiv \sigma_{\rm rel}$, where $\sigma_{\rm rel}$ represents the intrinsic relative dispersion of neutrino momentum. The $\exp(-\lambda_{\rm ij})$ therm corresponds to the conventional quantum decoherence effect caused by the gradual separation of different mass states traveling at different spatial propagation speeds, which causes them to stop interfering with each other, leading to damped oscillations. The terms containing y_{ij} describe the dispersion effect, which includes two effects on the oscillations: wave packet spreading compensates for wave packet separation, and dispersion reduces the overlap fraction of the wave packets [21, 25]. The $\exp(-\eta_{\text{ij}})$ term corresponds to the quantum decoherence effect from delocalization, which is related to the neutrino production and detection processes and is independent of the baseline L. We find that $\exp(-\eta_{\text{ij}})$ is very close to 1 at JUNO if $\sigma_{\text{rel}} \gtrsim \mathrm{O}(10^{-15})$. In ref. [22], the Daya Bay (DYB) collaboration published their first experimental limits, which are $10^{-14} < \sigma_{\text{rel}} < 0.23$ and $2.38 \times 10^{-17} < \sigma_{\text{rel}} < 0.23$ at a 95% CL when the dimensions of the reactor cores and detectors are and are not considered as constraints, respectively. Therefore, we neglect the $\exp(-\eta_{\text{ij}})$ term in eq. (2.2) in this work in the following text.[1]

In addition, some works have discussed exponential damping models such as $\exp\left(-\alpha\frac{L^2}{(2E)^2}\right)$ and $\exp\left(-\alpha\frac{(\Delta m^2_{\text{ij}})^2 L}{E^2}\right)$. The former was adopted in ref. [13] to approximately describe the mixing of three active neutrinos and a very light sterile neutrino in short-baseline reactor neutrino experiments. Here, α represents the magnitude of mixing between the three active neutrinos and the light sterile neutrino. Note that this approximate relationship does not hold for medium- or long-baseline neutrino experiments with an eV-scale sterile neutrino or for mixing scenarios involving three active neutrinos and multiple sterile neutrinos. The latter damping model was proposed to explain the decoherence effect caused by quantum gravity in the Super-Kamiokande experiment [64], and the coupling α can be related to M_{Planck}. For a single-baseline experiment or an experiment with multiple identical baselines, the phenomenology of the former model above is the same as that of the type (1) model, and the phenomenology of the latter model above is the same as that of the type (7) model. Therefore, we will not discuss these two models in depth in this paper.

3 Damping signatures at medium-baseline reactor neutrino experiments

In this section, we first discuss the damping effects on the survival probability of $\bar{\nu}_e$ in medium-baseline reactor neutrino experiments. After that, we classify the damping effects in accordance with their different damping behaviors.

3.1 Damped neutrino oscillation probabilities

From the general expression in eq. (2.1), we can obtain four cases for the damped survival probability of reactor neutrinos ($\bar{\nu}_e$) in vacuum, as follows:

(I) The overall $\bar{\nu}_e$ survival probability is damped out. This case includes the QD I, QD II, QD III, and absorption damping effects.

$$\begin{aligned} P(\bar{\nu}_e \to \bar{\nu}_e) = D\{1 - c^4_{13}\sin^2(2\theta_{12})\sin^2(\Delta_{21}) - c^2_{12}\sin^2(2\theta_{13})\sin^2(\Delta_{31}) \\ - s^2_{12}\sin^2(2\theta_{13})\sin^2(\Delta_{32})\}, \end{aligned} \tag{3.1}$$

---

[1] If we consider the decoherence effect caused by delocalization, the lower limit on σ_{rel} at JUNO can reach 3.0×10^{-17} at 95% CL. Although this expected lower limit is slightly better than the DYB limit of $\sigma_{\text{rel}} > 2.38 \times 10^{-17}$, the improvement from JUNO is not large due to the smaller IBD events compared with DYB and the baseline independence of delocalization [22].

where the expression in curly brackets represents the $\bar{\nu}_e$ survival probability in vacuum without damping effects (i.e., the standard $\bar{\nu}_e$ survival probability), $D = D_{\rm ij}$ because there are no relevant $\Delta m^2_{\rm ij}$ terms in these damping factors, $c_{\rm ij} = \cos\theta_{\rm ij}$, $s_{\rm ij} = \sin\theta_{\rm ij}$, and the oscillation phase $\Delta_{\rm ij}$ is defined as

$$\Delta_{\rm ij} = \frac{\Delta m^2_{\rm ij} L}{4E} \simeq 1.267\frac{\Delta m^2_{\rm ij}[\mathrm{eV}^2]L[\mathrm{km}]}{E[\mathrm{GeV}]} = 1.267\frac{\Delta m^2_{\rm ij}[\mathrm{eV}^2]L[\mathrm{m}]}{E[\mathrm{MeV}]}. \tag{3.2}$$

(II) Some oscillating and nonoscillating terms of the $\bar{\nu}_e$ survival probability are damped out. This case includes the ν_3 decay damping effect.

$$\begin{aligned} P(\bar{\nu}_e \to \bar{\nu}_e) = {} & c^4_{13}[1 - \sin^2(2\theta_{12})\sin^2(\Delta_{21})] \\ & + \frac{1}{2}\sin^2(2\theta_{13})\exp\left(-\frac{\alpha L}{2E}\right)[c^2_{12}\cos(2\Delta_{31}) + s^2_{12}\cos(2\Delta_{32})] \\ & + \exp\left(-\frac{\alpha L}{E}\right)s^4_{13}. \end{aligned} \tag{3.3}$$

(III) Only the oscillating terms of the $\bar{\nu}_e$ survival probability are damped out, but there are no dispersion terms. This case includes the WPD I and WPD II damping effects.

$$\begin{aligned} P(\bar{\nu}_e \to \bar{\nu}_e) = 1 & - \frac{1}{2}[c^4_{13}\sin^2(2\theta_{12}) + \sin^2(2\theta_{13})] + \frac{1}{2}c^4_{13}\sin^2(2\theta_{12})D_{21}\cos(2\Delta_{21}) \\ & + \frac{1}{2}\sin^2(2\theta_{13})[D_{31}c^2_{12}\cos(2\Delta_{31}) + D_{32}s^2_{12}\cos(2\Delta_{32})]. \end{aligned} \tag{3.4}$$

(IV) Not only are the oscillating terms of the $\bar{\nu}_e$ survival probability damped out, but there are also dispersion terms. This case includes the WPD III damping effect.

$$\begin{aligned} P(\bar{\nu}_e \to \bar{\nu}_e) = 1 & - \frac{1}{2}c^4_{13}\sin^2(2\theta_{12})\left[1 - \left(\frac{1}{1+y^2_{21}}\right)^{\frac{1}{4}}\exp(-\lambda_{21})\cos(\phi_{21})\right] \\ & - \frac{1}{2}\sin^2(2\theta_{13})c^2_{12}\left[1 - \left(\frac{1}{1+y^2_{31}}\right)^{\frac{1}{4}}\exp(-\lambda_{31})\cos(\phi_{31})\right] \\ & - \frac{1}{2}\sin^2(2\theta_{13})s^2_{12}\left[1 - \left(\frac{1}{1+y^2_{32}}\right)^{\frac{1}{4}}\exp(-\lambda_{32})\cos(\phi_{32})\right], \end{aligned} \tag{3.5}$$

where $\phi_{\rm ij} = \frac{\Delta m^2_{\rm ij} L}{2E} + \frac{1}{2}\arctan(y_{\rm ij}) - \lambda_{\rm ij} y_{\rm ij}$ and is the sum of the plane wave phase and the phase shift introduced by wave packet dispersion.

In general, the $\bar{\nu}_e$ survival probability at JUNO is also affected by the Mikheyev-Smirnov-Wolfenstein (MSW) matter effect as the neutrinos travel through matter [65, 66]. We can treat this damping effect as a minor perturbation of the neutrino oscillations in matter [13]. For the standard three-neutrino oscillation scenarios, the corrections to the neutrino parameters due to matter effects do not exceed 1.1% [11, 67, 68]. In this work, we also ignore matter effects because they only slightly shift the central values of the neutrino oscillation parameters and do not affect the measurement precision.

3.2 Classification of damping effects

In figure 1, we plot the $\bar{\nu}_e$ survival probability $P(\bar{\nu}_e \to \bar{\nu}_e)$ with different damping parameter values for each new physics model. The neutrino oscillation parameters are taken from ref. [4] and summarized in table 2. We assume the NMO in this analysis. We find that the results are quite similar for the IMO. We choose a few values for the damping parameters for illustration. In particular, $\alpha = 0$ indicates no damping effect, i.e., neutrino oscillation of the standard type. The farther the spectrum is from the no-damping curve, the stronger the intensity of the damping effect. The distortion of the standard $\bar{\nu}_e$ survival probability spectrum caused by damping is a combined phenomenon of an amplitude decrease and a phase shift, which can be regarded as a unique signature, as shown in figure 1. We find that the amplitude decrease behaviors of both the fast oscillation cycles (driven by Δm^2_{31} and Δm^2_{32}) and the slow oscillation cycles (driven by Δm^2_{21}) are more significant than their phase shift behaviors in all damping effect scenarios. Therefore, damping effects mainly smear the fine structure of the standard $\bar{\nu}_e$ survival probability spectrum through amplitude-decreasing effects. Furthermore, the fine structure of the fast oscillation cycles is smeared more strongly than that of the slow oscillation cycles with increasing α, which indicates that more spectral shape information is lost in the former than in the latter.

Based on the different smearing behaviors, we can divide the damping effects in table 1 into three categories. The first category is referred to as the QD-like effects, which include the QD I, QD II, QD III, and absorption damping effects. Although the details of the smearing behavior of each model are different, the fine structure is more completely preserved under increasing α for models in this category than for models in the other two categories. As $\alpha \to \infty$, the $\bar{\nu}_e$ survival probabilities of the models in this category approach zero, which means that the neutrinos do not propagate. The second category includes the ν_3 decay effect. In this category, the fine structure of the fast oscillation cycles will be smeared more strongly as α increases until all details of the fast oscillation structure are lost. However, the damping effects of this category will not affect the fine structure of the slow oscillation cycles. Consequently, only the slow oscillation cycles will remain as $\alpha \to \infty$. The third category is referred to as WPD-like effects, which include the WPD I, WPD II, and WPD III damping effects. As α increases, the fine structures of both the fast and slow oscillation cycles will be strongly smeared under WPD-like effects, but the former will be smeared out before the latter. The $\bar{\nu}_e$ survival probabilities of these models approach a nonzero constant value as $\alpha \to \infty$, i.e., $1 - \frac{1}{2}[c^4_{13} \sin^2(2\theta_{12}) + \sin^2(2\theta_{13})]$. Notably, the number of neutrinos will be lost in the damping models of the first and second categories, whereas they will keep the same in the third category.

4 Analysis method for JUNO

The damping effects on the reactor neutrino oscillations can be probed at JUNO by measuring the distortion of the neutrino inverse beta decay (IBD) event spectrum. The observed $\bar{\nu}_e$ distribution in terms of the reconstructed energy (E_{rec}) can be expressed as

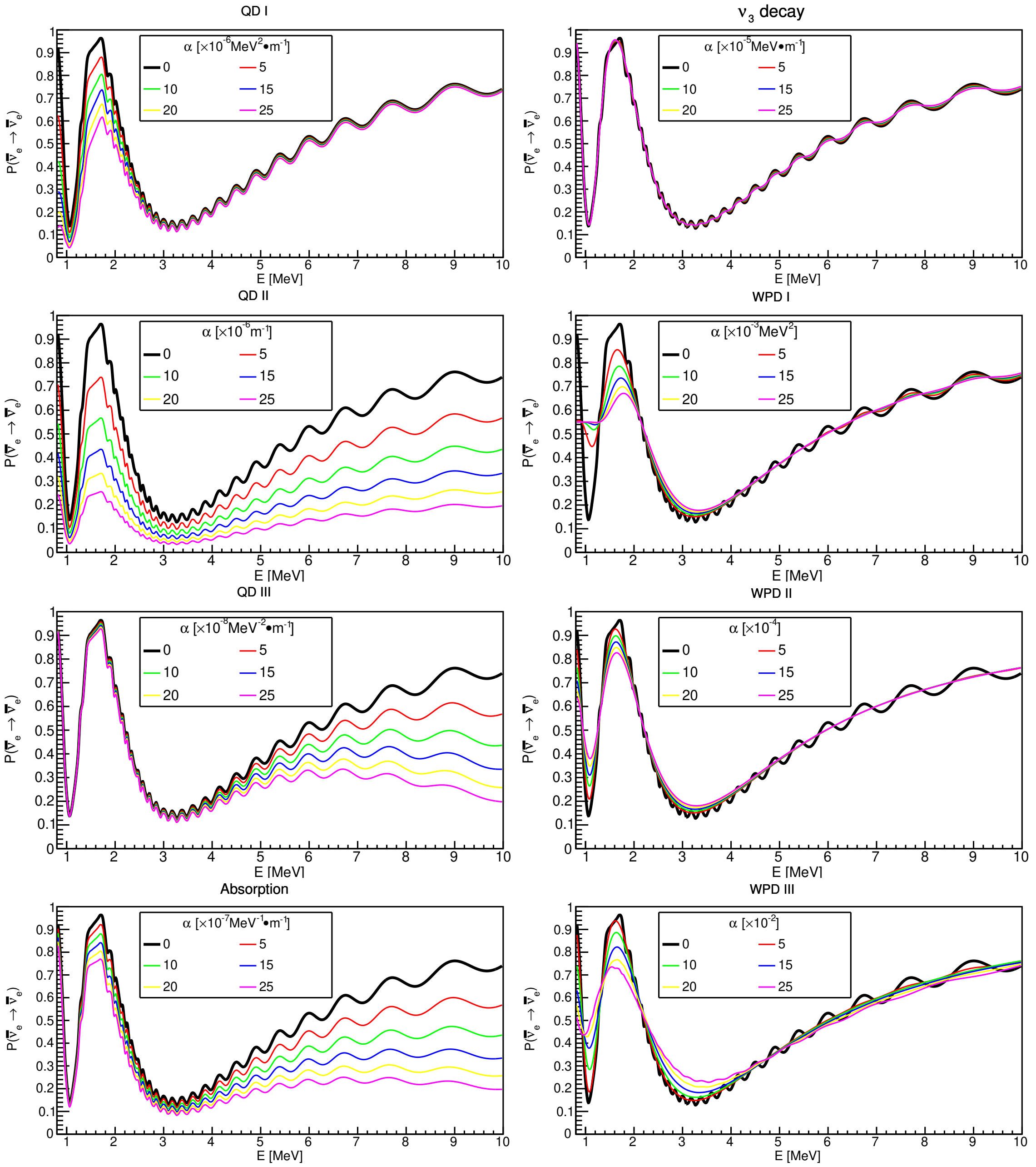

Figure 1. The $\bar{\nu}_e$ survival probability $P(\bar{\nu}_e \rightarrow \bar{\nu}_e)$ with different damping parameter values for each new physics model.

p	$\sin^2\theta_{12}$	$\sin^2\theta_{13}$	$\Delta m^2_{21}(\mathrm{eV}^2)$	$\Delta m^2_{32}(\mathrm{NMO}, \mathrm{eV}^2)$	$\Delta m^2_{32}(\mathrm{IMO}, \mathrm{eV}^2)$
p^{input}	0.307	2.18×10^{-2}	7.53×10^{-5}	2.453×10^{-3}	-2.546×10^{-3}
δp	0.013	0.07×10^{-2}	0.18×10^{-5}	0.034×10^{-3}	0.037×10^{-3}

Table 2. The neutrino oscillation parameters used in this work [4]. The input values p^{input} and the corresponding 1σ uncertainty values δp are taken from ref. [4]. For the case in which Δm^2_{32} is negative, the corresponding δp is the average value.

follows [69]:

$$\frac{dN}{dE_{\mathrm{rec}}} = \frac{N_{\mathrm{p}}T}{4\pi L^2}\int_{m_n - m_p + m_e} dE \frac{W_{\mathrm{th}}}{\sum_u f_u \varpi_u}\sum_u f_u S_u(E) P(\bar{\nu}_e \to \bar{\nu}_e)\sigma_{\mathrm{IBD}}(E) G(E_{\mathrm{vis}} - E_{\mathrm{rec}}, \delta E_{\mathrm{vis}}), \tag{4.1}$$

where N_{p} is the total number of free target protons in the LS detector, T is the total exposure time, and W_{th} is the thermal power of the reactor. f_u, ϖ_u, and S_u are the fission fraction, the mean energy released per fission, and the $\bar{\nu}_e$ energy spectrum per fission, respectively, for the isotope u, where $u = \{^{235}\mathrm{U},\ ^{238}\mathrm{U},\ ^{239}\mathrm{Pu},\ ^{241}\mathrm{Pu}\}$. The values of f_u and ϖ_u are taken from ref. [70]. $S_{^{235}\mathrm{U}}$, $S_{^{239}\mathrm{Pu}}$, and $S_{^{241}\mathrm{Pu}}$ are derived from ref. [71], and $S_{^{238}\mathrm{U}}$ is derived from ref. [72]. $\sigma_{\mathrm{IBD}}(E)$ is the cross section for IBD in a detector, taken from refs. [73, 74]; E_{vis} is the visible energy ($E_{\mathrm{vis}} \sim E_e + m_e \sim (E - 0.8)$ MeV), and $G(E_{\mathrm{vis}} - E_{\mathrm{rec}}, \delta E_{\mathrm{vis}})$ is a normalized Gaussian function representing a detector response function with an energy resolution of δE_{vis}. This function is expressed as follows:

$$G(E_{\mathrm{vis}} - E_{\mathrm{rec}}, \delta E_{\mathrm{vis}}) \approx \frac{1}{\sqrt{2\pi}\delta E_{\mathrm{vis}}} \exp\left\{-\frac{(E_{\mathrm{vis}} - E_{\mathrm{rec}})^2}{2(\delta E_{\mathrm{vis}})^2}\right\}, \tag{4.2}$$

where δE_{vis} is taken from ref. [11]. The detector energy resolution can be described by a three-parameter function, i.e.,

$$\frac{\delta E_{\mathrm{vis}}}{E_{\mathrm{vis}}} = \sqrt{\left(\frac{p_0}{\sqrt{E_{\mathrm{vis}}/\mathrm{MeV}}}\right)^2 + p_1^2 + \left(\frac{p_2}{E_{\mathrm{vis}}/\mathrm{MeV}}\right)^2}, \tag{4.3}$$

where the parameters p_0, p_1 and p_2 represent the contributions to the energy resolution from the photon statistics, detector-related residual energy nonuniformity, and photomultiplier tube (PMT)-related effects, respectively.

The effective energy resolution of 3% at 1 MeV of the JUNO detector, as discussed in refs. [12, 75], is considered, and we set $p_0 = 2.61\%$, $p_1 = 0.82\%$, and $p_2 = 1.23\%$. We also take the IBD detection efficiency of the detector to be 73% [11, 75]. The JUNO detector is located at equal distances of $\sim$ 53 km from the Yangjiang and Taishan thermal power reactor complexes [11, 12, 75]. The thermal powers of these two reactor complexes are 17.4 $\mathrm{GW_{th}}$ and 9.2 $\mathrm{GW_{th}}$, respectively [75]. We consider the exposure of the JUNO detector to be $(26.6 \times 20 \times 6 \times 300)$ $\mathrm{GW_{th}} \cdot \mathrm{kton} \cdot \mathrm{years} \cdot \mathrm{days}$ and assume the NMO scenario unless explicitly stated otherwise.

For the analysis, we adopt the least square method from refs. [11, 16, 18, 69, 76, 77] and define a χ^2 function with proper nuisance parameters and penalty terms to quantify the sensitivity of α, as follows:

$$\begin{aligned}\chi^2 = &\sum_i^{N_{\text{bin}}} \frac{\left[M_i - T_i\left(1+\epsilon_R+\epsilon_d+\sum_r \omega_r \epsilon_r + \epsilon_s\right) - \sum_b B_{b,i}(1+\epsilon_b)\right]^2}{T_i + (\sigma^{\text{shape}} T_i)^2 + \sum_b (B_{b,i}\sigma_b^{\text{shape}})^2} \\ &+ \frac{\epsilon_R^2}{\sigma_R^2} + \frac{\epsilon_d^2}{\sigma_d^2} + \sum_r \frac{\epsilon_r^2}{\sigma_r^2} + \frac{\epsilon_s^2}{\sigma_s^2} + \sum_b \frac{\epsilon_b^2}{\sigma_b^2} \\ &+ \sum_k \left(\frac{p_k^{\text{input}} - p_k^{\text{fit}}}{\delta p_k}\right)^2 ,\end{aligned} \tag{4.4}$$

where N_{bin} is the number of energy bins, M_i is the number of measured total events (the summation of signal and background) in the i-th bin, T_i is the predicted number of IBD events, B_b is the b-th kind of estimated background (the main background spectra for the JUNO detector are taken from ref. [11]), and the quantities σ and ϵ with different indices represent systematic uncertainties and the corresponding pull parameters, respectively. The considered systematic uncertainties include the correlated reactor uncertainty (σ_R=2%), the detector-related uncertainty (σ_d=1%), the uncorrelated reactor uncertainty (σ_r=0.8%), the uncorrelated spectrum shape uncertainty (σ_s=1%), the correlated spectrum shape uncertainty (σ^{shape}=1%), the shape uncertainties of the backgrounds (σ_b^{shape}), and the relative rate uncertainties of the backgrounds (σ_b). Specifically, the σ_b^{shape} values for accidental coincidences, fast neutrons, ^{9}Li/^{8}He, ^{13}C(α, n)^{16}O and geoneutrinos at JUNO are negligible (i.e., 0%), 20%, 10%, 50%, and 5%, respectively; the corresponding σ_b values are 1%, 100%, 20%, 50%, and 30%, respectively. Additionally, ω_r is a fraction representing the r-th reactor's contribution to the corresponding pull parameter ϵ_r. Finally, p_k and δp_k denote the k-th neutrino oscillation parameter ($\sin^2\theta_{12}$, $\sin^2\theta_{13}$, Δm^2_{21}, or $\Delta \mathrm{m}^2_{32}$) and the corresponding uncertainty, respectively, at a 1σ CL; these values are given in table 2.

5 Results

In this section, we present the results of probing the damping signatures of different new physics models at JUNO. We firstly study the constraints on the damping parameters for the eight new physics models at JUNO. Then, we show that JUNO can also help to disentangle the damping model from each other.

5.1 Constraints on the damping parameters at JUNO

To obtain the constraints on the damping parameters at JUNO, we scan the damping parameter of each damping model by marginalizing over other parameters, and fit the simulated no-damping JUNO data to obtain the exclusion sensitivities of the damping parameters. We list the constraints on the damping parameter of each damping model from this work in table 3. The current bounds on the damping parameters in the literature are also listed for comparison. The damping factors of the first seven damping models in

Damping type Parameter [units]	Phenomenological limits (experiment: original results, CL [Ref]) {Experimental limits (experiment: original results, CL [Ref])}	Exclusion sensitivities for JUNO (CL)
QD I α [$\times 10^{-6}\ \frac{\mathrm{MeV}^2}{\mathrm{m}}$]	$< 1.62 \times 10^5$ (MINOS+T2K+reactor: $\alpha < 3.2 \times 10^{-23}$ GeV^3, 90% [33]) < 0.41 (solar+KL: $\alpha < 0.81 \times 10^{-28}$ GeV^3, 95% [20])	< 3.72 (90%) < 4.42 (95%)
QD II α [$\times \frac{10^{-6}}{\mathrm{m}}$]	< 3.45 (KL: 6.8×10^{-22} GeV, 95% [40]) < 0.33 (MINOS+T2K+reactor: $\alpha < 6.5 \times 10^{-23}$ GeV, 90% [33]) < 0.18 (SK: $\alpha < 3.5 \times 10^{-23}$ GeV, 90% [35]) $< 3.40 \times 10^{-3}$ (solar+KL: $\alpha < 0.67 \times 10^{-24}$ GeV, 95% [20])	< 0.80 (90%) < 0.95 (95%)
QD III α [$\times \frac{10^{-8}}{\mathrm{MeV}^2 \cdot \mathrm{m}}$]	$< 2.38 \times 10^{-3}$(solar+KL: $\alpha < 0.47 \times 10^{-20}$ GeV^{-1}, 95% [20]) $< 1.42 \times 10^{-5}$ (MINOS+T2K+reactor: $\alpha < 2.8 \times 10^{-23}$ GeV^{-1}, 90% [33]) $< 4.56 \times 10^{-10}$ (SK: $\alpha < 0.9 \times 10^{-27}$ GeV^{-1}, 90% [35])	< 1.22 (90%) < 1.46 (95%)
Absorption α [$\times \frac{10^{-7}}{\mathrm{MeV} \cdot \mathrm{m}}$]	< 7.60 (KL: $\alpha < 1.5 \times 10^{-19}$, 95% [40]) < 0.10 (SK: $\alpha < 2.0 \times 10^{-21}$, 90% [35]) $< 2.94 \times 10^{-3}$ (solar+KL: $\alpha < 0.58 \times 10^{-22}$, 95% [20])	< 1.04 (90%) < 1.23 (95%)
ν_3 decay $\alpha \equiv \frac{m_3}{\tau_3}$ [$\times 10^{-4}\ \frac{\mathrm{MeV}}{\mathrm{m}}$]	< 256.59 (OPERA: $\frac{\tau_3}{m_3} > 1.3 \times 10^{-13}\ \frac{\mathrm{s}}{\mathrm{eV}}$, 90% [43]) < 22.24 (NOνA+T2K: $\frac{\tau_3}{m_3} > 1.5 \times 10^{-12}\ \frac{\mathrm{s}}{\mathrm{eV}}$, 90% [17]) < 0.36 (SK+K2K+MINOS: $\frac{\tau_3}{m_3} > 9.3 \times 10^{-11}\ \frac{\mathrm{s}}{\mathrm{eV}}$, 99% [41]) {$< 15.88$ (MINOS: $\frac{\tau_3}{m_3} > 2.1 \times 10^{-12}\ \frac{\mathrm{s}}{\mathrm{eV}}$, 90% [15])}	< 0.44 (90%) < 0.53 (95%) < 0.75 (99%)
WPD I $\alpha \equiv (4\sqrt{2}\sigma_x)^{-2}$ [$\times 10^{-3}$MeV^2]	< 116.96 (RENO+DYB: $\sigma_x > 1.02 \times 10^{-4}$ nm, 90% [24]) < 27.59 (RENO+DYB+KL: $\sigma_x > 2.1 \times 10^{-4}$ nm, 90% [49])	< 0.18 (90%) < 0.22 (95%)
WPD II α [$\times 10^{-4}$]		< 0.14 (95%)
WPD III $\alpha \equiv \sigma_{\mathrm{rel}}$ [$\times 10^{-2}$]	{< 23 (DYB: $\sigma_{\mathrm{rel}} < 0.23$, 95% [22])}	< 1.04 (95%)
$\sigma_x \equiv (2\alpha E)^{-1}$ [$\times 10^{-3}$ nm]	{$> 10^{-1}$ (DYB: $\sigma_x > 10^{-4}$ nm, 95% [22])}	> 2.32 (95%)

Table 3. The limits on the damping parameters for each damping model at JUNO. The experimental and phenomenological limits in the literature are also shown for comparison.

table 3 can be unified into a general form [13, 14],

$$D_{\mathrm{ij}} = \exp\left(-\alpha \frac{|\Delta m^2_{\mathrm{ij}}|^{\xi} L^{\beta}}{E^{\gamma}}\right), \tag{5.1}$$

where the parameters ξ, β, and γ are the power numbers in the damping factor of interest. The strength of neutrino oscillation experiments to probe the damping effects is strongly dependent on the specific values of ξ, β, and γ [13, 14].

Compared to current experimental limits, we find that JUNO will improve the limits on τ_3/m_3 in the ν_3 decay model by a factor of ~ 36. The limits on σ_{rel} (or σ_x) in the WPD III

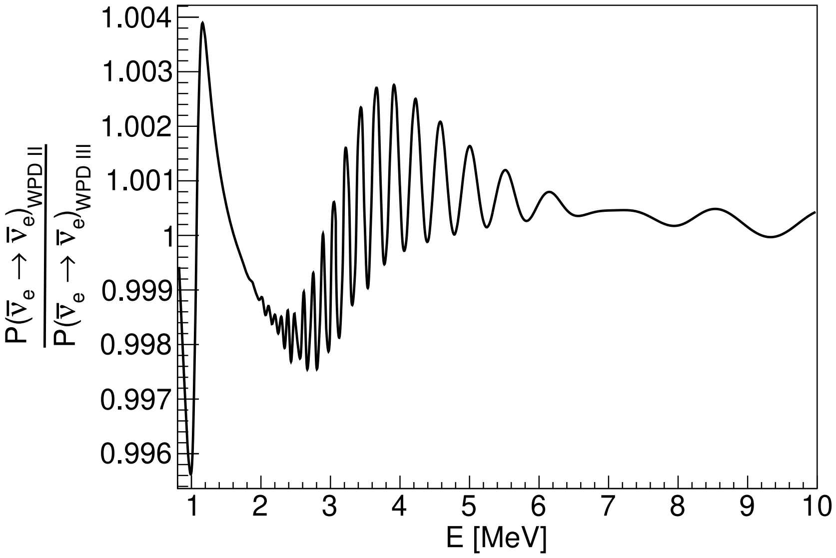

Figure 2. The ratio of the $\bar{\nu}_e$ survival probabilities between the WPD II and WPD III scenarios as a function of the neutrino energy. Here the oscillation parameters are taken from table 2 and the damping parameter $\sigma_{\rm rel}$ is set to 2.08×10^{-2}, which corresponds to a 5σ CL limit obtained from this work.

model can be also improved by a factor of ~ 22 (23). After taking into account the previous limits from phenomenological analysis, we find that JUNO will also impose stronger limits on the damping parameters in WPD I and WPD III. However, the improvement of the bounds on the damping parameters in the QD I, QD II, QD III, ν_3 decay and neutrino absorption scenarios from JUNO is not significant compared to other phenomenological analysis. This is mainly due to the fact that JUNO has a smaller value of $|\Delta m^2_{\rm ij}|^\xi L^\beta / E^\gamma$. From table 3, we see that a global joint analysis can be more restrictive in terms of these limits, which provides a promising future direction for JUNO to study these damping effects.

In the WPD II model, we also replace α with $(\sqrt{2}\sigma_{\rm rel}/4)^2$ to study the effect of limit on $\sigma_{\rm rel}$ in the absence of the quantum decoherence caused by the dispersion effect. We find that the upper limits on $\sigma_{\rm rel}$ for the WPD II and WPD III are about the same, which means that the quantum decoherence caused by the dispersion effect is negligible on the limits on the damping parameters at JUNO. This can be understood from figure 2, which shows that the $\bar{\nu}_e$ survival probabilities described by eq. (3.4) and eq. (3.5) are very close at JUNO, and the modification to the $\bar{\nu}_e$ survival probability due to the dispersion effect is less than 0.5%.

5.2 Disentangling damping signatures at JUNO

To compare these eight damping effects, we follow the analysis method described in ref. [13]. For a fixed set of oscillation parameters and α values in the simulated damping model, we marginalize over the oscillation parameters, α values and all pull parameters in the fitted model. Then, we define a threshold $\alpha_{\rm th}$ as the sensitivity limit for the simulated α, i.e., the simulated α must be above this threshold for the simulated damping model to be

JUNO 95% (3σ)	Simulated damping model							
Fitted model	QD I $\frac{\alpha}{10^{-6}\,\frac{\mathrm{MeV}^2}{\mathrm{m}}} \gtrsim$	QD II $\frac{\alpha}{\frac{10^{-6}}{\mathrm{m}}} \gtrsim$	QD III $\frac{\alpha}{\frac{10^{-8}}{\mathrm{MeV}^2\bullet\mathrm{m}}} \gtrsim$	Absorption $\frac{\alpha}{\frac{10^{-7}}{\mathrm{MeV}\bullet\mathrm{m}}} \gtrsim$	ν_3 decay $\frac{\alpha}{10^{-4}\,\frac{\mathrm{MeV}}{\mathrm{m}}} \gtrsim$	WPD I $\frac{\alpha}{10^{-3}\mathrm{MeV}^2} \gtrsim$	WPD II $\frac{\alpha}{10^{-4}} \gtrsim$	WPD III $\frac{\alpha}{10^{-2}} \gtrsim$
No damping	4.62 (7.2)	0.99 (1.54)	1.51 (2.35)	1.28 (1.99)	0.55 (0.93)	0.22 (0.44)	0.14 (0.24)	1.05 (1.39)
QD I	—	1.05 (1.62)	1.51 (2.35)	1.28 (1.99)	0.55 (0.93)	0.22 (0.44)	0.14 (0.24)	1.05 (1.39)
QD II	4.82 (7.5)	—	1.75 (2.71)	1.84 (2.84)	0.55 (0.93)	0.22 (0.44)	0.14 (0.24)	1.05 (1.39)
QD III	4.62 (7.2)	1.16 (1.8)	—	4.54 (7.16)	0.55 (0.93)	0.22 (0.44)	0.14 (0.24)	1.05 (1.39)
Absorption	4.62 (7.2)	1.43 (2.24)	5.26 (8.21)	—	0.55 (0.93)	0.22 (0.44)	0.14 (0.24)	1.05 (1.39)
ν_3 decay	4.62 (7.2)	0.99 (1.54)	1.51 (2.35)	1.28 (1.99)	—	4.03 (7.17)	10.48 (16.64)	8.88 (11.04)
WPD I	4.62 (7.2)	0.99 (1.54)	1.51 (2.35)	1.28 (1.99)	4.4 (-)	—	3.2 (39.2)	4.72 (15.68)
WPD II	4.62 (7.2)	0.99 (1.54)	1.51 (2.35)	1.28 (1.99)	—	10 (17.2)	—	21.76 (25.04)
WPD III	4.62 (7.2)	0.99 (1.54)	1.51 (2.35)	1.28 (1.99)	—	9.12 (15.68)	66.8 (88.4)	—

Table 4. The sensitivity limits on α for which a certain simulated damping model (in columns) could be distinguished from a certain fitted model (in rows) at JUNO.

distinguishable from the fitted model at JUNO. The corresponding sensitivity limits at a 95% (3σ) CL obtained through this work are shown in table 4, where we specifically include the no-damping model among the fitted models. For instance, the QD I model could be distinguished from the no-damping model at the 95% CL if $\alpha \gtrsim 4.62 \times 10^{-6}$ MeV^2/m.

In the rows representing ν_3 decay versus WPD-like models, there are no corresponding α_{th} values at the 3σ CL since the χ^2 are below 6.4 for all α values in the simulated ν_3 decay model. This can be attributed to the distortion of the standard $\bar{\nu}_e$ survival probability spectrum caused by the ν_3 decay, which can be easily compensated for by shifting the neutrino oscillation parameters and α in the fitted WPD-like models. In the columns representing WPD-like models, the values with other WPD-like or ν_3 decay scenarios are several orders of magnitude greater than the values with QD-like models. Thus, if a WPD-like model exists in nature, it will be much more difficult to distinguish it from other WPD-like scenarios or from a ν_3 decay scenario as compared to a QD-like model.

6 Conclusions

In this paper, we systematically study the phenomenology of damping signatures at JUNO, a medium-baseline reactor neutrino oscillation experiment. As the benchmark models in this work, we analyze several new physics scenarios, including quantum decoherence, ν_3 decay, neutrino absorption, and wave packet decoherence. Based on a six-year exposure and five main background sources for the JUNO detector, we demonstrate how to test and disentangle the fine-scale spectral structure caused by the damping effects. The exclusion sensitivities on the damping parameters at JUNO for each benchmark model are listed in table 3. Compared to current experimental limits, JUNO will significantly improve the limits on τ_3/m_3 in the ν_3 decay model, the width of the neutrino wave packet σ_x, and the intrinsic relative dispersion of neutrino momentum $\sigma_{\rm rel}$ by a factor of $\sim$ 36, 23 and 22, respectively. Furthermore, we find that the quantum decoherence caused by the dispersion effect is negligible at JUNO. Finally, we find that compared to the QD-like models, the WPD-like and ν_3 decay models are much more difficult to distinguish from each other at JUNO.

Acknowledgments

We are grateful for the ongoing cooperation from the China General Nuclear Power Group. This work was supported by the Chinese Academy of Sciences, the National Key R&D Program of China, the CAS Center for Excellence in Particle Physics, Wuyi University, and the Tsung-Dao Lee Institute of Shanghai Jiao Tong University in China, the Institut National de Physique Nucléaire et de Physique des Particulest (IN2P3) in France, the Istituto Nazionale di Fisica Nucleare (INFN) in Italy, the Italian-Chinese collaborative research program MAECI-NSFC, the Fond de la Recherche Scientifique (F.R.S-FNRS) and FWO under the "Excellence of Science — EOS" in Belgium, the Conselho Nacional de Desenvolvimento Científico e Tecnològico in Brazil, the Agencia Nacional de Investigacion y Desarrollo in Chile, the Charles University Research Centre and the Ministry of Education, Youth, and Sports in Czech Republic, the Deutsche Forschungsgemeinschaft (DFG), the Helmholtz Association, and the Cluster of Excellence PRISMA+ in Germany, the Joint Institute of Nuclear Research (JINR) and Lomonosov Moscow State University in Russia, the joint Russian Science Foundation (RSF) and National Natural Science Foundation of China (NSFC) research program, the MOST and MOE in Taiwan, the Chulalongkorn University and Suranaree University of Technology in Thailand, and the University of California at Irvine in U.S.A.

References

[1] B. Pontecorvo, *Inverse beta processes and nonconservation of lepton charge*, *Zh. Eksp. Teor. Fiz.* **34** (1957) 247 [INSPIRE].

[2] SUPER-KAMIOKANDE collaboration, *Evidence for oscillation of atmospheric neutrinos*, *Phys. Rev. Lett.* **81** (1998) 1562 [`hep-ex/9807003`] [INSPIRE].

- [3] C. Giganti, S. Lavignac and M. Zito, *Neutrino oscillations: The rise of the PMNS paradigm*, *Prog. Part. Nucl. Phys.* **98** (2018) 1 [`arXiv:1710.00715`] [INSPIRE].
- [4] Particle Data Group collaboration, *Review of Particle Physics*, *PTEP* **2020** (2020) 083C01 [INSPIRE].
- [5] NOvA collaboration, *Measurement of the neutrino mixing angle θ_{23} in NOvA*, *Phys. Rev. Lett.* **118** (2017) 151802 [`arXiv:1701.05891`] [INSPIRE].
- [6] Super-Kamiokande collaboration, *Atmospheric neutrino oscillation analysis with external constraints in Super-Kamiokande I-IV*, *Phys. Rev. D* **97** (2018) 072001 [`arXiv:1710.09126`] [INSPIRE].
- [7] T2K collaboration, *Constraint on the matter-antimatter symmetry-violating phase in neutrino oscillations*, *Nature* **580** (2020) 339 [*Erratum ibid.* **583** (2020) E16] [`arXiv:1910.03887`] [INSPIRE].
- [8] DUNE collaboration, *Long-Baseline Neutrino Facility (LBNF) and Deep Underground Neutrino Experiment (DUNE): Conceptual Design Report, Volume 2: The Physics Program for DUNE at LBNF*, `arXiv:1512.06148` [INSPIRE].
- [9] DUNE collaboration, *Long-baseline neutrino oscillation physics potential of the DUNE experiment*, *Eur. Phys. J. C* **80** (2020) 978 [`arXiv:2006.16043`] [INSPIRE].
- [10] Hyper-Kamiokande collaboration, *Hyper-Kamiokande Design Report*, `arXiv:1805.04163` [INSPIRE].
- [11] JUNO collaboration, *Neutrino Physics with JUNO*, *J. Phys. G* **43** (2016) 030401 [`arXiv:1507.05613`] [INSPIRE].
- [12] JUNO collaboration, *JUNO Physics and Detector*, `arXiv:2104.02565` [INSPIRE].
- [13] M. Blennow, T. Ohlsson and W. Winter, *Damping signatures in future neutrino oscillation experiments*, *JHEP* **06** (2005) 049 [`hep-ph/0502147`] [INSPIRE].
- [14] M. Blennow, *Damping signatures in future neutrino oscillation experiments*, *Nucl. Phys. B Proc. Suppl.* **155** (2006) 195 [INSPIRE].
- [15] MINOS collaboration, *Search for sterile neutrino mixing in the MINOS long baseline experiment*, *Phys. Rev. D* **81** (2010) 052004 [`arXiv:1001.0336`] [INSPIRE].
- [16] T. Abrahão, H. Minakata, H. Nunokawa and A.A. Quiroga, *Constraint on Neutrino Decay with Medium-Baseline Reactor Neutrino Oscillation Experiments*, *JHEP* **11** (2015) 001 [`arXiv:1506.02314`] [INSPIRE].
- [17] S. Choubey, D. Dutta and D. Pramanik, *Invisible neutrino decay in the light of NOvA and T2K data*, *JHEP* **08** (2018) 141 [`arXiv:1805.01848`] [INSPIRE].
- [18] Y.P. Porto-Silva, S. Prakash, O.L.G. Peres, H. Nunokawa and H. Minakata, *Constraining visible neutrino decay at KamLAND and JUNO*, *Eur. Phys. J. C* **80** (2020) 999 [`arXiv:2002.12134`] [INSPIRE].
- [19] A. Ghoshal, A. Giarnetti and D. Meloni, *Neutrino Invisible Decay at DUNE: a multi-channel analysis*, *J. Phys. G* **48** (2021) 055004 [`arXiv:2003.09012`] [INSPIRE].
- [20] G.L. Fogli, E. Lisi, A. Marrone, D. Montanino and A. Palazzo, *Probing non-standard decoherence effects with solar and KamLAND neutrinos*, *Phys. Rev. D* **76** (2007) 033006 [`arXiv:0704.2568`] [INSPIRE].
- [21] Y.-L. Chan, M.C. Chu, K.M. Tsui, C.F. Wong and J. Xu, *Wave-packet treatment of reactor neutrino oscillation experiments and its implications on determining the neutrino mass hierarchy*, *Eur. Phys. J. C* **76** (2016) 310 [`arXiv:1507.06421`] [INSPIRE].

[22] Daya Bay collaboration, *Study of the wave packet treatment of neutrino oscillation at Daya Bay*, *Eur. Phys. J. C* **77** (2017) 606 [arXiv:1608.01661] [inSPIRE].

[23] J.A.B. Coelho, W.A. Mann and S.S. Bashar, *Nonmaximal θ_{23} mixing at NOvA from neutrino decoherence*, *Phys. Rev. Lett.* **118** (2017) 221801 [arXiv:1702.04738] [inSPIRE].

[24] A. de Gouvêa, V. de Romeri and C.A. Ternes, *Probing neutrino quantum decoherence at reactor experiments*, *JHEP* **08** (2020) 018 [arXiv:2005.03022] [inSPIRE].

[25] Z. Cheng, W. Wang, C.F. Wong and J. Zhang, *Studying the neutrino wave-packet effects at medium-baseline reactor neutrino oscillation experiments and the potential benefits of an extra detector*, *Nucl. Phys. B* **964** (2021) 115304 [arXiv:2009.06450] [inSPIRE].

[26] Y. Liu, J.-L. Chen and M.-L. Ge, *A constraint on EHNS parameters from solar neutrino problem*, *J. Phys. G* **24** (1998) 2289 [hep-ph/9711381] [inSPIRE].

[27] S. Shafaq, T. Kushwaha and P. Mehta, *Investigating Leggett-Garg inequality in neutrino oscillations — role of decoherence and decay*, arXiv:2112.12726 [inSPIRE].

[28] N.C. Ribeiro, H. Nunokawa, T. Kajita, S. Nakayama, P. Ko and H. Minakata, *Probing Nonstandard Neutrino Physics by Two Identical Detectors with Different Baselines*, *Phys. Rev. D* **77** (2008) 073007 [arXiv:0712.4314] [inSPIRE].

[29] Y. Farzan, T. Schwetz and A.Y. Smirnov, *Reconciling results of LSND, MiniBooNE and other experiments with soft decoherence*, *JHEP* **07** (2008) 067 [arXiv:0805.2098] [inSPIRE].

[30] P.A.N. Machado, H. Nunokawa, F.A. Pereira dos Santos and R. Zukanovich Funchal, *Testing Nonstandard Neutrino Properties with a Mössbauer Oscillation Experiment*, *JHEP* **11** (2011) 136 [arXiv:1108.3339] [inSPIRE].

[31] R.L.N. de Oliveira, M.M. Guzzo and P.C. de Holanda, *Quantum Dissipation and CP Violation in MINOS*, *Phys. Rev. D* **89** (2014) 053002 [arXiv:1401.0033] [inSPIRE].

[32] P. Coloma, J. Lopez-Pavon, I. Martinez-Soler and H. Nunokawa, *Decoherence in Neutrino Propagation Through Matter, and Bounds from IceCube/DeepCore*, *Eur. Phys. J. C* **78** (2018) 614 [arXiv:1803.04438] [inSPIRE].

[33] A.L.G. Gomes, R.A. Gomes and O.L.G. Peres, *Quantum decoherence and relaxation in neutrinos using long-baseline data*, arXiv:2001.09250 [inSPIRE].

[34] Y. Liu, L.-z. Hu and M.-L. Ge, *The effect of quantum mechanics violation on neutrino oscillation*, *Phys. Rev. D* **56** (1997) 6648 [inSPIRE].

[35] E. Lisi, A. Marrone and D. Montanino, *Probing possible decoherence effects in atmospheric neutrino oscillations*, *Phys. Rev. Lett.* **85** (2000) 1166 [hep-ph/0002053] [inSPIRE].

[36] D. Morgan, E. Winstanley, J. Brunner and L.F. Thompson, *Probing quantum decoherence in atmospheric neutrino oscillations with a neutrino telescope*, *Astropart. Phys.* **25** (2006) 311 [astro-ph/0412618] [inSPIRE].

[37] N.E. Mavromatos and S. Sarkar, *Methods of approaching decoherence in the flavour sector due to space-time foam*, *Phys. Rev. D* **74** (2006) 036007 [hep-ph/0606048] [inSPIRE].

[38] P. Mehta and W. Winter, *Interplay of energy dependent astrophysical neutrino flavor ratios and new physics effects*, *JCAP* **03** (2011) 041 [arXiv:1101.2673] [inSPIRE].

[39] P. Bakhti, Y. Farzan and T. Schwetz, *Revisiting the quantum decoherence scenario as an explanation for the LSND anomaly*, *JHEP* **05** (2015) 007 [arXiv:1503.05374] [inSPIRE].

[40] G. Balieiro Gomes, M.M. Guzzo, P.C. de Holanda and R.L.N. Oliveira, *Parameter Limits for Neutrino Oscillation with Decoherence in KamLAND*, *Phys. Rev. D* **95** (2017) 113005 [arXiv:1603.04126] [inSPIRE].

[41] M.C. Gonzalez-Garcia and M. Maltoni, *Status of Oscillation plus Decay of Atmospheric and Long-Baseline Neutrinos*, *Phys. Lett. B* **663** (2008) 405 [`arXiv:0802.3699`] [INSPIRE].

[42] R.A. Gomes, A.L.G. Gomes and O.L.G. Peres, *Constraints on neutrino decay lifetime using long-baseline charged and neutral current data*, *Phys. Lett. B* **740** (2015) 345 [`arXiv:1407.5640`] [INSPIRE].

[43] G. Pagliaroli, N. Di Marco and M. Mannarelli, *Enhanced tau neutrino appearance through invisible decay*, *Phys. Rev. D* **93** (2016) 113011 [`arXiv:1603.08696`] [INSPIRE].

[44] C. Giunti, C.W. Kim and U.W. Lee, *Coherence of neutrino oscillations in vacuum and matter in the wave packet treatment*, *Phys. Lett. B* **274** (1992) 87 [INSPIRE].

[45] C. Giunti and C.W. Kim, *Coherence of neutrino oscillations in the wave packet approach*, *Phys. Rev. D* **58** (1998) 017301 [`hep-ph/9711363`] [INSPIRE].

[46] C. Giunti, *Coherence and wave packets in neutrino oscillations*, *Found. Phys. Lett.* **17** (2004) 103 [`hep-ph/0302026`] [INSPIRE].

[47] M. Blasone, F. Dell'Anno, S. De Siena and F. Illuminati, *Flavor entanglement in neutrino oscillations in the wave packet description*, *EPL* **112** (2015) 20007 [`arXiv:1510.06761`] [INSPIRE].

[48] J. Kersten and A.Y. Smirnov, *Decoherence and oscillations of supernova neutrinos*, *Eur. Phys. J. C* **76** (2016) 339 [`arXiv:1512.09068`] [INSPIRE].

[49] A. de Gouvêa, V. De Romeri and C.A. Ternes, *Combined analysis of neutrino decoherence at reactor experiments*, *JHEP* **06** (2021) 042 [`arXiv:2104.05806`] [INSPIRE].

[50] T. Ohlsson, *Equivalence between neutrino oscillations and neutrino decoherence*, *Phys. Lett. B* **502** (2001) 159 [`hep-ph/0012272`] [INSPIRE].

[51] D.V. Naumov and V.A. Naumov, *A diagrammatic treatment of neutrino oscillations*, *J. Phys. G* **37** (2010) 105014 [`arXiv:1008.0306`] [INSPIRE].

[52] D.V. Naumov and V.A. Naumov, *Quantum Field Theory of Neutrino Oscillations*, *Phys. Part. Nucl.* **51** (2020) 1 [INSPIRE].

[53] J.R. Ellis, N.E. Mavromatos, D.V. Nanopoulos and E. Winstanley, *Quantum decoherence in a four-dimensional black hole background*, *Mod. Phys. Lett. A* **12** (1997) 243 [`gr-qc/9602011`] [INSPIRE].

[54] J.R. Ellis, N.E. Mavromatos and D.V. Nanopoulos, *Quantum decoherence in a D foam background*, *Mod. Phys. Lett. A* **12** (1997) 1759 [`hep-th/9704169`] [INSPIRE].

[55] M. Lindner, T. Ohlsson and W. Winter, *A combined treatment of neutrino decay and neutrino oscillations*, *Nucl. Phys. B* **607** (2001) 326 [`hep-ph/0103170`] [INSPIRE].

[56] A.S. Joshipura, E. Masso and S. Mohanty, *Constraints on decay plus oscillation solutions of the solar neutrino problem*, *Phys. Rev. D* **66** (2002) 113008 [`hep-ph/0203181`] [INSPIRE].

[57] J.F. Beacom and N.F. Bell, *Do Solar Neutrinos Decay?*, *Phys. Rev. D* **65** (2002) 113009 [`hep-ph/0204111`] [INSPIRE].

[58] G.L. Fogli, E. Lisi, A. Marrone and D. Montanino, *Status of atmospheric* $\nu_\mu \to \nu_\tau$ *oscillations and decoherence after the first K2K spectral data*, *Phys. Rev. D* **67** (2003) 093006 [`hep-ph/0303064`] [INSPIRE].

[59] P. Baerwald, M. Bustamante and W. Winter, *Neutrino Decays over Cosmological Distances and the Implications for Neutrino Telescopes*, *JCAP* **10** (2012) 020 [`arXiv:1208.4600`] [INSPIRE].

[60] R. Picoreti, M.M. Guzzo, P.C. de Holanda and O.L.G. Peres, *Neutrino Decay and Solar Neutrino Seasonal Effect*, *Phys. Lett. B* **761** (2016) 70 [`arXiv:1506.08158`] [INSPIRE].

[61] A.M. Gago, R.A. Gomes, A.L.G. Gomes, J. Jones-Perez and O.L.G. Peres, *Visible neutrino decay in the light of appearance and disappearance long baseline experiments*, *JHEP* **11** (2017) 022 [`arXiv:1705.03074`] [INSPIRE].

[62] SNO collaboration, *Constraints on Neutrino Lifetime from the Sudbury Neutrino Observatory*, *Phys. Rev. D* **99** (2019) 032013 [`arXiv:1812.01088`] [INSPIRE].

[63] E.K. Akhmedov and A.Y. Smirnov, *Paradoxes of neutrino oscillations*, *Phys. Atom. Nucl.* **72** (2009) 1363 [`arXiv:0905.1903`] [INSPIRE].

[64] S.L. Adler, *Comment on a proposed Super-Kamiokande test for quantum gravity induced decoherence effects*, *Phys. Rev. D* **62** (2000) 117901 [`hep-ph/0005220`] [INSPIRE].

[65] L. Wolfenstein, *Neutrino Oscillations in Matter*, *Phys. Rev. D* **17** (1978) 2369 [INSPIRE].

[66] S.P. Mikheyev and A.Y. Smirnov, *Resonance Amplification of Oscillations in Matter and Spectroscopy of Solar Neutrinos*, *Sov. J. Nucl. Phys.* **42** (1985) 913 [INSPIRE].

[67] Y.-F. Li, Y. Wang and Z.-z. Xing, *Terrestrial matter effects on reactor antineutrino oscillations at JUNO or RENO-50: how small is small?*, *Chin. Phys. C* **40** (2016) 091001 [`arXiv:1605.00900`] [INSPIRE].

[68] A.N. Khan, H. Nunokawa and S.J. Parke, *Why matter effects matter for JUNO*, *Phys. Lett. B* **803** (2020) 135354 [`arXiv:1910.12900`] [INSPIRE].

[69] S.-F. Ge, K. Hagiwara, N. Okamura and Y. Takaesu, *Determination of mass hierarchy with medium baseline reactor neutrino experiments*, *JHEP* **05** (2013) 131 [`arXiv:1210.8141`] [INSPIRE].

[70] Daya Bay collaboration, *Improved Measurement of the Reactor Antineutrino Flux and Spectrum at Daya Bay*, *Chin. Phys. C* **41** (2017) 013002 [`arXiv:1607.05378`] [INSPIRE].

[71] P. Huber, *On the determination of anti-neutrino spectra from nuclear reactors*, *Phys. Rev. C* **84** (2011) 024617 [*Erratum ibid.* **85** (2012) 029901] [`arXiv:1106.0687`] [INSPIRE].

[72] T.A. Mueller et al., *Improved Predictions of Reactor Antineutrino Spectra*, *Phys. Rev. C* **83** (2011) 054615 [`arXiv:1101.2663`] [INSPIRE].

[73] A. Strumia and F. Vissani, *Precise quasielastic neutrino/nucleon cross-section*, *Phys. Lett. B* **564** (2003) 42 [`astro-ph/0302055`] [INSPIRE].

[74] A.S. Dighe, M.T. Keil and G.G. Raffelt, *Detecting the neutrino mass hierarchy with a supernova at IceCube*, *JCAP* **06** (2003) 005 [`hep-ph/0303210`] [INSPIRE].

[75] JUNO collaboration, *Calibration Strategy of the JUNO Experiment*, *JHEP* **03** (2021) 004 [`arXiv:2011.06405`] [INSPIRE].

[76] F. Capozzi, E. Lisi and A. Marrone, *Neutrino mass hierarchy and electron neutrino oscillation parameters with one hundred thousand reactor events*, *Phys. Rev. D* **89** (2014) 013001 [`arXiv:1309.1638`] [INSPIRE].

[77] H. Wang, L. Zhan, Y.-F. Li, G. Cao and S. Chen, *Mass hierarchy sensitivity of medium baseline reactor neutrino experiments with multiple detectors*, *Nucl. Phys. B* **918** (2017) 245 [`arXiv:1602.04442`] [INSPIRE].

The JUNO collaboration

Jun Wang[1], Jiajun Liao[1,*], Wei Wang[1,*], Angel Abusleme[6], Thomas Adam[45], Shakeel Ahmad[66], Rizwan Ahmed[66], Sebastiano Aiello[55], Muhammad Akram[66], Fengpeng An[29], Qi An[22], Giuseppe Andronico[55], Nikolay Anfimov[67], Vito Antonelli[57], Tatiana Antoshkina[67], Burin Asavapibhop[71], João Pedro Athayde Marcondes de André[45], Didier Auguste[43], Andrej Babic[70], Nikita Balashov[67], Wander Baldini[56], Andrea Barresi[58], Davide Basilico[57], Eric Baussan[45], Marco Bellato[60], Antonio Bergnoli[60], Thilo Birkenfeld[48], Sylvie Blin[43], David Blum[54], Simon Blyth[40], Anastasia Bolshakova[67], Mathieu Bongrand[47], Clément Bordereau[44,40], Dominique Breton[43], Augusto Brigatti[57], Riccardo Brugnera[61], Riccardo Bruno[55], Antonio Budano[64], Mario Buscemi[55], Jose Busto[46], Ilya Butorov[67], Anatael Cabrera[43], Hao Cai[34], Xiao Cai[11], Yanke Cai[11], Zhiyan Cai[11], Riccardo Callegari[61], Antonio Cammi[59], Agustin Campeny[6], Chuanya Cao[11], Guofu Cao[11], Jun Cao[11], Rossella Caruso[55], Cédric Cerna[44], Jinfan Chang[11], Yun Chang[39], Pingping Chen[19], Po-An Chen[40], Shaomin Chen[14], Xurong Chen[26], Yi-Wen Chen[38], Yixue Chen[12], Yu Chen[1], Zhang Chen[11], Jie Cheng[11], Yaping Cheng[8], Alexey Chetverikov[67], Davide Chiesa[58], Pietro Chimenti[4], Artem Chukanov[67], Gérard Claverie[44], Catia Clementi[62], Barbara Clerbaux[3], Selma Conforti Di Lorenzo[44], Daniele Corti[60], Flavio Dal Corso[60], Olivia Dalager[74], Christophe De La Taille[44], Jiawei Deng[34], Zhi Deng[14], Ziyan Deng[11], Wilfried Depnering[52], Marco Diaz[6], Xuefeng Ding[57], Yayun Ding[11], Bayu Dirgantara[73], Sergey Dmitrievsky[67], Tadeas Dohnal[41], Dmitry Dolzhikov[67], Georgy Donchenko[69], Jianmeng Dong[14], Evgeny Doroshkevich[68], Marcos Dracos[45], Frédéric Druillole[44], Ran Du[11], Shuxian Du[37], Stefano Dusini[60], Martin Dvorak[41], Timo Enqvist[42], Heike Enzmann[52], Andrea Fabbri[64], Lukas Fajt[70], Donghua Fan[24], Lei Fan[11], Jian Fang[11], Wenxing Fang[11], Marco Fargetta[55], Dmitry Fedoseev[67], Vladko Fekete[70], Li-Cheng Feng[38], Qichun Feng[21], Richard Ford[57], Amélie Fournier[44], Haonan Gan[32], Feng Gao[48], Alberto Garfagnini[61], Arsenii Gavrikov[61], Marco Giammarchi[57], Agnese Giaz[61], Nunzio Giudice[55], Maxim Gonchar[67], Guanghua Gong[14], Hui Gong[14], Yuri Gornushkin[67], Alexandre Göttel[50,48], Marco Grassi[61], Christian Grewing[51], Vasily Gromov[67], Minghao Gu[11], Xiaofei Gu[37], Yu Gu[20], Mengyun Guan[11], Nunzio Guardone[55], Maria Gul[66], Cong Guo[11], Jingyuan Guo[1], Wanlei Guo[11], Xinheng Guo[9], Yuhang Guo[35,50], Paul Hackspacher[52], Caren Hagner[49], Ran Han[8], Yang Han[1], Muhammad Sohaib Hassan[66], Miao He[11], Wei He[11], Tobias Heinz[54], Patrick Hellmuth[44], Yuekun Heng[11], Rafael Herrera[6], YuenKeung Hor[1], Shaojing Hou[11], Yee Hsiung[40], Bei-Zhen Hu[40], Hang Hu[1], Jianrun Hu[11], Jun Hu[11], Shouyang Hu[10], Tao Hu[11], Zhuojun Hu[1], Chunhao Huang[1], Guihong Huang[11], Hanxiong Huang[10], Wenhao Huang[25], Xin Huang[11], Xingtao Huang[25], Yongbo Huang[28], Jiaqi Hui[30], Lei Huo[21], Wenju Huo[22], Cédric Huss[44], Safeer Hussain[66], Ara Ioannisian[2], Roberto Isocrate[60], Beatrice Jelmini[61], Kuo-Lun Jen[38], Ignacio Jeria[6], Xiaolu Ji[11], Xingzhao Ji[1], Huihui Jia[33], Junji Jia[34], Siyu Jian[10], Di Jiang[22], Wei Jiang[11], Xiaoshan Jiang[11], Ruyi Jin[11], Xiaoping Jing[11], Cécile Jollet[44], Jari Joutsenvaara[42], Sirichok Jungthawan[73], Leonidas Kalousis[45], Philipp Kampmann[50], Li Kang[19], Rebin Karaparambil[47], Narine Kazarian[2], Khanchai Khosonthongkee[73], Denis Korablev[67], Konstantin Kouzakov[69], Alexey Krasnoperov[67], Andre Kruth[51], Nikolay Kutovskiy[67], Pasi Kuusiniemi[42], Tobias Lachenmaier[54], Cecilia Landini[57], Sébastien Leblanc[44], Victor Lebrin[47], Frederic Lefevre[47], Ruiting Lei[19], Rupert Leitner[41], Jason Leung[38], Demin Li[37], Fei Li[11], Fule Li[14], Haitao Li[1], Huiling Li[11], Jiaqi Li[1], Mengzhao Li[11], Min Li[12], Nan Li[11], Nan Li[17], Qingjiang Li[17], Ruhui Li[11], Shanfeng Li[19], Tao Li[1], Weidong Li[11,15], Weiguo Li[11], Xiaomei Li[10], Xiaonan Li[11], Xinglong Li[10], Yi Li[19], Yufeng Li[11], Zhaohan Li[11], Zhibing Li[1], Ziyuan Li[1], Hao Liang[10], Hao Liang[22], Daniel Liebau[51], Ayut Limphirat[73], Sukit Limpijumnong[73], Guey-Lin Lin[38], Shengxin Lin[19], Tao Lin[11], Jiajie Ling[1], Ivano Lippi[60], Fang Liu[12], Haidong Liu[37], Hongbang Liu[28], Hongjuan Liu[23], Hongtao Liu[1], Hui Liu[20], Jianglai Liu[30,31], Jinchang Liu[11], Min Liu[23], Qian Liu[15], Qin Liu[22], Runxuan Liu[50,48], Shuangyu Liu[11], Shubin Liu[22], Shulin Liu[11], Xiaowei Liu[1], Xiwen Liu[28], Yan Liu[11], Yunzhe Liu[11], Alexey Lokhov[69,68], Paolo Lombardi[57], Claudio Lombardo[55], Kai Loo[52], Chuan Lu[32], Haoqi Lu[11], Jingbin Lu[16], Junguang Lu[11], Shuxiang Lu[37], Xiaoxu Lu[11], Bayarto Lubsandorzhiev[68], Sultim Lubsandorzhiev[68], Livia Ludhova[50,48], Arslan Lukanov[68], Fengjiao Luo[11], Guang Luo[1], Pengwei Luo[1], Shu Luo[36], Wuming Luo[11], Vladimir Lyashuk[68], Bangzheng Ma[25], Qiumei Ma[11], Si Ma[11], Xiaoyan Ma[11], Xubo Ma[12], Jihane Maalmi[43], Yury Malyshkin[67], Roberto Carlos Mandujano[74], Fabio Mantovani[56], Francesco Manzali[61], Xin Mao[8], Yajun Mao[13], Stefano M. Mari[64], Filippo Marini[61], Sadia Marium[66], Cristina Martellini[64], Gisele Martin-Chassard[43], Agnese Martini[63], Matthias Mayer[53], Davit Mayilyan[2], Ints Mednieks[65], Yue Meng[30], Anselmo Meregaglia[44], Emanuela Meroni[57], David Meyhöfer[49], Mauro Mezzetto[60], Jonathan Miller[7], Lino Miramonti[57], Paolo Montini[64], Michele Montuschi[56], Axel Müller[54], Massimiliano Nastasi[58], Dmitry V. Naumov[67], Elena Naumova[67], Diana Navas-Nicolas[43], Igor Nemchenok[67], Minh Thuan Nguyen Thi[38], Feipeng Ning[11], Zhe Ning[11], Hiroshi Nunokawa[5], Lothar Oberauer[53], Juan Pedro Ochoa-Ricoux[74,5], Alexander Olshevskiy[67], Domizia Orestano[64], Fausto Ortica[62], Rainer Othegraven[52], Hsiao-Ru Pan[40], Alessandro Paoloni[63], Sergio Parmeggiano[57], Yatian Pei[11], Nicomede Pelliccia[62], Anguo Peng[23], Haiping Peng[22], Frédéric Perrot[44], Pierre-Alexandre Petitjean[3], Fabrizio Petrucci[64], Oliver Pilarczyk[52], Luis Felipe Piñeres Rico[45], Artyom Popov[69], Pascal Poussot[45], Wathan Pratumwan[73], Ezio Previtali[58], Fazhi Qi[11], Ming Qi[27], Sen Qian[11], Xiaohui Qian[11], Zhen Qian[1], Hao Qiao[13], Zhonghua Qin[11], Shoukang Qiu[23], Muhammad Usman Rajput[66], Gioacchino Ranucci[57], Neill Raper[1], Alessandra Re[57], Henning Rebber[49], Abdel Rebii[44], Bin Ren[19], Jie Ren[10], Barbara Ricci[56], Markus Robens[51], Mathieu Roche[44], Narongkiat Rodphai[71], Aldo Romani[62], Bedřich Roskovec[41], Christian Roth[51], Xiangdong Ruan[28], Xichao Ruan[10], Saroj Rujirawat[73], Arseniy Rybnikov[67], Andrey Sadovsky[67], Paolo Saggese[57], Simone Sanfilippo[64], Anut Sangka[72], Nuanwan Sanguansak[73], Utane Sawangwit[72], Julia Sawatzki[53], Fatma Sawy[61], Michaela Schever[50,48], Cédric Schwab[45], Konstantin Schweizer[53], Alexandr Selyunin[67], Andrea Serafini[56], Giulio Settanta[50], Mariangela Settimo[47], Zhuang Shao[35], Vladislav Sharov[67], Arina Shaydurova[67], Jingyan Shi[11], Yanan Shi[11], Vitaly Shutov[67], Andrey Sidorenkov[68], Fedor Šimkovic[70], Chiara Sirignano[61], Jaruchit Siripak[73], Monica Sisti[58], Maciej Slupecki[42], Mikhail Smirnov[1], Oleg Smirnov[67], Thiago Sogo-Bezerra[47], Sergey Sokolov[67], Julanan Songwadhana[73], Boonrucksar Soonthornthum[72], Albert Sotnikov[67], Ondřej Šrámek[41], Warintorn Sreethawong[73], Achim Stahl[48], Luca Stanco[60], Konstantin Stankevich[69], Dušan Štefánik[70], Hans Steiger[52,53], Jochen Steinmann[48], Tobias Sterr[54], Matthias Raphael Stock[53], Virginia Strati[56], Alexander Studenikin[69], Shifeng Sun[12], Xilei Sun[11], Yongjie Sun[22], Yongzhao Sun[11], Narumon Suwonjandee[71], Michal Szelezniak[45], Jian Tang[1], Qiang Tang[1], Quan Tang[23], Xiao Tang[11], Alexander Tietzsch[54], Igor Tkachev[68], Tomas Tmej[41], Marco Danilo Claudio Torri[41], Konstantin Treskov[67], Andrea Triossi[45], Giancarlo Troni[6], Wladyslaw Trzaska[42], Cristina Tuve[55], Nikita Ushakov[68], Johannes van den Boom[51], Stefan van Waasen[51], Guillaume Vanroyen[47], Vadim Vedin[65], Giuseppe Verde[55], Maxim Vialkov[69], Benoit Viaud[47], Cornelius Moritz Vollbrecht[50,48], Cristina Volpe[43], Vit Vorobel[41], Dmitriy Voronin[68], Lucia Votano[63], Pablo Walker[6], Caishen Wang[19], Chung-Hsiang Wang[39], En Wang[37], Guoli Wang[21], Jian Wang[22], Kunyu Wang[11], Lu Wang[11], Meifen Wang[11], Meng Wang[23], Meng Wang[25], Ruiguang Wang[11], Siguang Wang[13], Wei Wang[27], Wenshuai Wang[11], Xi Wang[17], Xiangyue Wang[1], Yangfu Wang[11], Yaoguang Wang[11], Yi Wang[14], Yi Wang[24], Yifang Wang[11], Yuanqing Wang[14], Yuman Wang[27], Zhe Wang[14], Zheng Wang[11], Zhimin Wang[11], Zongyi Wang[14], Muhammad Waqas[66], Apimook Watcharangkool[72], Lianghong Wei[11], Wei Wei[11], Wenlu Wei[11], Yadong Wei[19], Kaile Wen[11], Liangjian Wen[11], Christopher Wiebusch[48], Steven Chan-Fai Wong[1], Bjoern Wonsak[49], Diru Wu[11], Qun Wu[25], Zhi Wu[11], Michael Wurm[52], Jacques Wurtz[45], Christian Wysotzki[48], Yufei Xi[32], Dongmei Xia[18], Xiaochuan Xie[18], Yuguang Xie[11], Zhangquan Xie[11], Zhizhong Xing[11], Benda Xu[14], Cheng Xu[23], Donglian Xu[31,30], Fanrong Xu[20], Hangkun Xu[11], Jilei Xu[11], Jing Xu[9], Meihang Xu[11], Yin Xu[33], Yu Xu[50,48], Baojun Yan[11], Taylor Yan[73], Wenqi Yan[11], Xiongbo Yan[11], Yupeng Yan[73], Anbo Yang[11], Changgen Yang[11], Chengfeng Yang[28], Huan Yang[11], Jie Yang[37], Lei Yang[19], Xiaoyu Yang[11], Yifan Yang[11], Yifan Yang[3], Haifeng Yao[11], Zafar Yasin[66], Jiaxuan Ye[11], Mei Ye[11], Ziping Ye[31], Ugur Yegin[51], Frédéric Yermia[47], Peihuai Yi[11], Na Yin[25], Xiangwei Yin[11], Zhengyun You[1], Boxiang Yu[11], Chiye Yu[19], Chunxu Yu[33], Hongzhao Yu[1], Miao Yu[34], Xianghui Yu[33], Zeyuan Yu[11], Zezhong Yu[11], Chengzhuo Yuan[11], Ying Yuan[13], Zhenxiong Yuan[14], Ziyi Yuan[34], Baobiao Yue[1], Noman Zafar[66], Andre Zambanini[51], Vitalii Zavadskyi[67], Shan Zeng[11], Tingxuan Zeng[11], Yuda Zeng[1], Liang Zhan[11], Aiqiang Zhang[14], Feiyang Zhang[30], Guoqing Zhang[11], Haiqiong Zhang[11], Honghao Zhang[1], Jiawen Zhang[11], Jie Zhang[11], Jin Zhang[28], Jingbo Zhang[21], Jinnan Zhang[11], Peng Zhang[11], Qingmin Zhang[35], Shiqi Zhang[1], Shu Zhang[1], Tao Zhang[30], Xiaomei Zhang[11], Xuantong Zhang[11], Xueyao Zhang[25], Yan Zhang[11], Yinhong Zhang[11], Yiyu Zhang[11], Yongpeng Zhang[11], Yuanyuan Zhang[30], Yumei Zhang[1], Zhenyu Zhang[34], Zhijian Zhang[19], Fengyi Zhao[26], Jie Zhao[11], Rong Zhao[1], Shujun Zhao[37], Tianchi Zhao[11], Dongqin Zheng[20], Hua Zheng[19], Minshan Zheng[10], Yangheng Zheng[15], Weirong Zhong[20], Jing Zhou[10], Li Zhou[11], Nan Zhou[22], Shun Zhou[11], Tong Zhou[11], Xiang Zhou[34], Jiang Zhu[1], Kangfu Zhu[35], Kejun Zhu[11], Zhihang Zhu[11], Bo Zhuang[11], Honglin Zhuang[11], Liang Zong[14], Jiaheng Zou[11],

[*] *Corresponding author*
[1] *Sun Yat-Sen University, Guangzhou, China*
[2] *Yerevan Physics Institute, Yerevan, Armenia*
[3] *Université Libre de Bruxelles, Brussels, Belgium*
[4] *Universidade Estadual de Londrina, Londrina, Brazil*
[5] *Pontificia Universidade Catolica do Rio de Janeiro, Rio, Brazil*
[6] *Pontificia Universidad Católica de Chile, Santiago, Chile*
[7] *Universidad Tecnica Federico Santa Maria, Valparaiso, Chile*
[8] *Beijing Institute of Spacecraft Environment Engineering, Beijing, China*
[9] *Beijing Normal University, Beijing, China*
[10] *China Institute of Atomic Energy, Beijing, China*
[11] *Institute of High Energy Physics, Beijing, China*
[12] *North China Electric Power University, Beijing, China*
[13] *School of Physics, Peking University, Beijing, China*
[14] *Tsinghua University, Beijing, China*
[15] *University of Chinese Academy of Sciences, Beijing, China*
[16] *Jilin University, Changchun, China*
[17] *College of Electronic Science and Engineering, National University of Defense Technology, Changsha, China*
[18] *Chongqing University, Chongqing, China*
[19] *Dongguan University of Technology, Dongguan, China*
[20] *Jinan University, Guangzhou, China*
[21] *Harbin Institute of Technology, Harbin, China*
[22] *University of Science and Technology of China, Hefei, China*
[23] *The Radiochemistry and Nuclear Chemistry Group in University of South China, Hengyang, China*
[24] *Wuyi University, Jiangmen, China*
[25] *Shandong University, Jinan, China, and Key Laboratory of Particle Physics and Particle Irradiation of Ministry of Education, Shandong University, Qingdao, China*
[26] *Institute of Modern Physics, Chinese Academy of Sciences, Lanzhou, China*

[27] Nanjing University, Nanjing, China
[28] Guangxi University, Nanning, China
[29] East China University of Science and Technology, Shanghai, China
[30] School of Physics and Astronomy, Shanghai Jiao Tong University, Shanghai, China
[31] Tsung-Dao Lee Institute, Shanghai Jiao Tong University, Shanghai, China
[32] Institute of Hydrogeology and Environmental Geology, Chinese Academy of Geological Sciences, Shijiazhuang, China
[33] Nankai University, Tianjin, China
[34] Wuhan University, Wuhan, China
[35] Xi'an Jiaotong University, Xi'an, China
[36] Xiamen University, Xiamen, China
[37] School of Physics and Microelectronics, Zhengzhou University, Zhengzhou, China
[38] Institute of Physics, National Yang Ming Chiao Tung University, Hsinchu
[39] National United University, Miao-Li
[40] Department of Physics, National Taiwan University, Taipei
[41] Charles University, Faculty of Mathematics and Physics, Prague, Czech Republic
[42] University of Jyvaskyla, Department of Physics, Jyvaskyla, Finland
[43] IJCLab, Université Paris-Saclay, CNRS/IN2P3, 91405 Orsay, France
[44] Univ. Bordeaux, CNRS, LP2i Bordeaux, UMR 5797, F-33170 Gradignan, France
[45] IPHC, Université de Strasbourg, CNRS/IN2P3, F-67037 Strasbourg, France
[46] Aix-Marseille Univ, CNRS/IN2P3, CPPM, Marseille, France
[47] SUBATECH, Nantes Université, IMT Atlantique, CNRS-IN2P3, Nantes, France
[48] III. Physikalisches Institut B, RWTH Aachen University, Aachen, Germany
[49] Institute of Experimental Physics, University of Hamburg, Hamburg, Germany
[50] Forschungszentrum Jülich GmbH, Nuclear Physics Institute IKP-2, Jülich, Germany
[51] Forschungszentrum Jülich GmbH, Central Institute of Engineering, Electronics and Analytics — Electronic Systems (ZEA-2), Jülich, Germany
[52] Institute of Physics, Johannes-Gutenberg Universität Mainz, Mainz, Germany
[53] Technische Universität München, München, Germany
[54] Eberhard Karls Universität Tübingen, Physikalisches Institut, Tübingen, Germany
[55] INFN Catania and Dipartimento di Fisica e Astronomia dell Università di Catania, Catania, Italy
[56] Department of Physics and Earth Science, University of Ferrara and INFN Sezione di Ferrara, Ferrara, Italy
[57] INFN Sezione di Milano and Dipartimento di Fisica dell Università di Milano, Milano, Italy
[58] INFN Milano Bicocca and University of Milano Bicocca, Milano, Italy
[59] INFN Milano Bicocca and Politecnico of Milano, Milano, Italy
[60] INFN Sezione di Padova, Padova, Italy
[61] Dipartimento di Fisica e Astronomia dell'Università di Padova and INFN Sezione di Padova, Padova, Italy
[62] INFN Sezione di Perugia and Dipartimento di Chimica, Biologia e Biotecnologie dell'Università di Perugia, Perugia, Italy
[63] Laboratori Nazionali di Frascati dell'INFN, Roma, Italy
[64] University of Roma Tre and INFN Sezione Roma Tre, Roma, Italy
[65] Institute of Electronics and Computer Science, Riga, Latvia
[66] Pakistan Institute of Nuclear Science and Technology, Islamabad, Pakistan
[67] Joint Institute for Nuclear Research, Dubna, Russia
[68] Institute for Nuclear Research of the Russian Academy of Sciences, Moscow, Russia
[69] Lomonosov Moscow State University, Moscow, Russia
[70] Comenius University Bratislava, Faculty of Mathematics, Physics and Informatics, Bratislava, Slovakia
[71] Department of Physics, Faculty of Science, Chulalongkorn University, Bangkok, Thailand
[72] National Astronomical Research Institute of Thailand, Chiang Mai, Thailand
[73] Suranaree University of Technology, Nakhon Ratchasima, Thailand
[74] Department of Physics and Astronomy, University of California, Irvine, California, U.S.A.